JOURNAL OF CATALYSIS 107, 82–91 (1987)

Study of the Carburization of an Iron Catalyst during the Fischer–Tropsch Synthesis: Influence on Its Catalytic Activity

M. PIJOLAT,[1] V. PERRICHON,[2] AND P. BUSSIÈRE

Institut de Recherches sur la Catalyse, Laboratoire Propre du CNRS conventionné à l'Université Claude Bernard Lyon I, 2 Avenue Albert Einstein, 69626 Villeurbanne Cedex, France

Received September 4, 1985; revised February 20, 1987

The fast transformation of an iron/alumina catalyst into $Fe_{2+x}C$ during the H_2 + CO reaction was followed by *in situ* Mössbauer spectroscopy at 523 K and the behavior was compared with changes in catalytic activity for Fischer–Tropsch synthesis. After a few hours of synthesis, no metallic iron could be detected by either Mössbauer or IR spectroscopy, whereas the CO conversion was still half of that observed initially. The nature of the sites responsible for the remaining activity is discussed. The interpretation of the Mössbauer spectra has permitted the determination of the stoichiometry of the $Fe_{2+x}C$ carbide ($0 \leq x \leq 0.4$), and hence the following of the change of x during the reaction. Thus, the activity in CO hydrogenation could be related to the number of carbon vacancies in the iron carbide, i.e., to the extent of the metallic character of this carbide. This concept of the variation of hydrogenating properties of the carbide with the carbon content has been supported by similar catalytic results obtained in the room temperature hydrogenation of ethylene performed on carbides of different stoichiometry.

1. INTRODUCTION

The transition metal carbides often exhibit catalytic properties different from those of the parent transition metal. In several reactions such as isomerization, hydrogenation, dehydrogenation, oxidation, and the Fischer–Tropsch (FT) synthesis, their activity is lower, sometimes by several orders of magnitude, but their selectivity may present interesting features (*1–3*). This has been explained by a modification of the band structure of the transition metal due to electron transfer between the metal and the carbon atoms. Controversy about the direction of the transfer still exists, but the current interpretation is that the metal acts as an electron donor (*3*). The transition metal carbides (and similarly the nitrides) can be considered interstitial compounds containing vacancies of the nonmetal atoms over a broad range of concentration, which results in a wide range of nonstoichiometric phases. As a consequence, their catalytic properties (as well as other properties) may be expected to vary accordingly. This has been shown experimentally for several carbides and nitrides of the metals of Groups IV, V, and VI, leading to the conclusion that the catalytic activity increases with the increasing number of nonmetal vacancies, that is with the degree of filling of the metal–metal bonding orbitals (*4–6*).

Until now, the carbides have been compared with the parent metals. However, in reactions involving carbon-containing molecules, the carbide phase may be a by-product of the reaction itself. This is the case with the FT reaction in which the initial metallic iron of an iron-based catalyst is progressively converted to a single phase or a mixture of iron carbide phases. At the same time, the catalytic activity is modified. Thus, depending upon the rate of carburization, the activity may either pass through a maximum which is related to the formation of the carbide (*7–9*), or in the

[1] Present address: ENS Mines, 158 Cours Fauriel, 42023 Saint Etienne, France.

[2] To whom correspondence should be addressed.

0021-9517/87 $3.00

case of rapid carburization it may simply decrease (*10–12*).

The characterization of the various stages of carburization is generally effected by means of *in situ* Mössbauer spectroscopy. In previous studies (*12, 13*), we have pointed out the need of a very careful interpretation of the literature data concerning the hyperfine parameters of iron carbides before the assignment of the spectral components to particular carbide phases. We have shown that the iron carbides may be classified as follows:

—"O carbides" in which the carbon atoms are located at octahedral sites of a hcp lattice of iron atoms, with a stoichiometry $Fe_{2+x}C$ where $0 \leq x \leq 0.4$ (e.g., "ε-Fe_2C", "ε'-$Fe_{2.2}C$").

—"TP carbides" in which the carbon atoms are located at the trigonal prismatic sites of more complicated structures for the iron lattice (e.g., θ-Fe_3C, χ-Fe_5C_2).

Moreover, we have shown that for iron catalysts supported on alumina, the overall stoichiometry of the $Fe_{2+x}C$ carbide varies continuously during the FT reaction. The differences in the reaction conditions and in the nature of the catalysts explain the large variety of carbide phases (or mixed phases) reported in the FT synthesis and the large stoichiometry range actually encountered.

In this paper, we have investigated the relationship which may exist between the catalytic properties of the iron "O carbides" and their stoichiometry. The starting material is an alumina-supported reduced iron catalyst. The activity decrease in the FT synthesis at 523 K is first discussed on the basis of the $Fe_{2+x}C$ carbide stoichiometry determined by *in situ* Mössbauer spectroscopy. Then, we present the results obtained in the hydrogenation of ethylene at room temperature with carbides of different stoichiometries (prepared by performing the FT synthesis for various times). Finally, we discuss the controversial question of the role of the iron carbides in the FT reaction and relate our experimental results to the general conclusions on the catalytic properties of the transition metal carbides.

2. EXPERIMENTAL

2.1. Catalyst

The catalyst consisted of 10 wt% iron supported on Al_2O_3 (Degussa Oxyd C) and was prepared by precipitation with Na_2CO_3 from an $FeCl_2/FeCl_3$ solution containing the alumina in suspension. The resulting mixture was briefly boiled and the precipitate was washed, before being dried at 378 K (*14*). Prior to reaction, the catalyst was reduced in the reactor cell by flowing hydrogen (SV = 5200 h^{-1}) for 18 h at 873 K, and subsequently cooled under H_2 at the desired reaction temperature.

2.2. Catalytic Reactions

The catalytic activities in the FT reaction and ethylene hydrogenation reaction were measured at atmospheric pressure in a differential flow reactor. In the case of the FT reaction, the outlet stream was heated at ~370 K. The products were analyzed by gas chromatography: CO, CO_2, and H_2 on a Porapak Q column (TCD); C_1 to C_{12} hydrocarbons on a SE 30 column (FID); and ethylene, ethane on a Porapak R column (FID).

The FT reaction conditions were 0.4 g of catalyst, SV = 1300 h^{-1}, and $H_2/CO = 1$. The ethylene hydrogenation was performed with the same loading and with a total flow rate of 1.8 l h^{-1}. The reaction mixture, $5H_2/1C_2H_4$, was diluted with helium in a ratio of 1 : 3.

2.3. In Situ Mössbauer Spectroscopy

Transmission Mössbauer spectra were obtained with a constant acceleration spectrometer operated in the triangular mode, with a 100 mCi $^{57}Co/Rh$ source. After computer folding, the spectra were fitted by using a least-squares program assuming Lorentzian-shaped lines. The calibration was achieved by means of an iron foil spectrum.

The isomer shifts δ are reported here with respect to sodium nitroprusside; the precision is 0.02 mm s^{-1}. The precision on quadrupole splittings Δ is 0.03 mm s^{-1} and that on hyperfine fields H is 2 kOe.

The sample, in the form of a pressed pellet (0.2 g), was placed in a heating cell equipped with two beryllium windows. It could be reduced *in situ* and treated with H_2 + CO under the conditions used in the catalytic test.

3. RESULTS AND DISCUSSION

3.1. Evolution of the Properties of the Catalyst during the Fischer–Tropsch Reaction

Figure 1 (*15*) illustrates the variations with time of the CO conversion toward hydrocarbons at different temperatures (473, 498, 523, and 548 K). The first product analysis was performed 5 min after the introduction of the reactants. The main

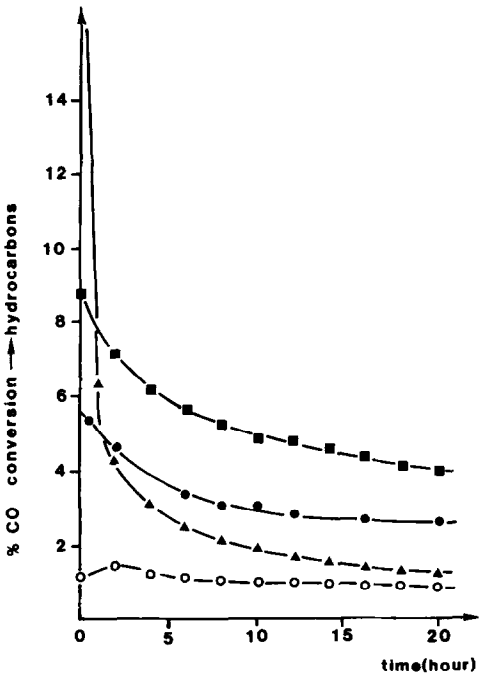

FIG. 1. Change in the activity of the reduced Fe/Al_2O_3 catalyst in the course of Fischer–Tropsch synthesis (*15*). (○) 473 K, (●) 498 K, (■) 523 K, (▲) 548 K.

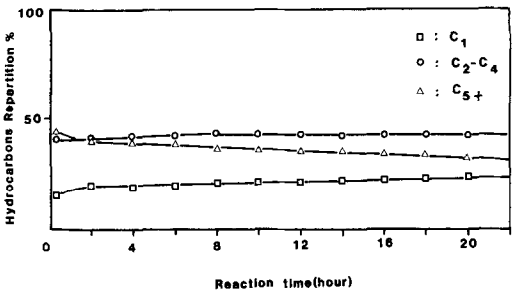

FIG. 2. Hydrocarbon distribution during Fischer–Tropsch synthesis over a reduced Fe/Al_2O_3 catalyst at 523 K.

relevant points may be summarized as follows.

With the exception of the reaction at 473 K where a slight maximum is observed after 3 h of synthesis, the activity decreases rapidly during the first hours of reaction. After that period, the decay of activity is slower. Under our conditions (1 atm pressure), no steady state is obtained even after 60 h at 523 K. At 548 K, the initial deactivation is rapid, which results in a final activity significantly lower than that observed, after 20 h, at 523 or 498 K.

The hydrocarbon distribution varies with the time of reaction, but much less so than with the temperature. The main changes occur during the first hours, where the methane selectivity increases at the expense of the higher hydrocarbons (see Fig. 2 at 523 K).

In situ physicochemical studies (*16*), particularly infrared (IR) spectroscopy and thermo-programmed reduction under H_2 (TPR), have indicated the presence of "active" surface carbon, bulk carbon, and "less reactive" carbon, which play an important role in the overall activity, as well as the presence of formates and higher carboxylates, which exist on the alumina support and have only a secondary role in hydrocarbon formation.

Thus, the rapid aging observed at 548 K is due to the deposit of "less reactive" carbon as evidenced by a methane TPR peak at 680 K. Consequently, since this paper is focused on the role of the bulk

carbide, we have concentrated this study on the aging of the catalyst at 523 K.

3.2. *Characterization of the Iron by Mössbauer Spectroscopy*

After H_2 reduction at 873 K for 18 h, the sample was cooled to 523 K in hydrogen, and the spectra were recorded at this temperature under the conditions of the reaction $1H_2 + 1CO$, for periods of 1 and 2 h. The procedure allowed us to improve the statistics, and thus to follow precisely a change during the first hours of the reaction. Figure 3 represents the spectra obtained after 1, 3, 5, and 22 h of reaction. These values are defined by the middle of the acquisition time.

The initial reduced catalyst spectrum presents besides an α-Fe sextuplet, a doublet of Fe^{2+}, the spectral contribution of which remains unchanged during the reaction and close to 25% of the total absorption area (at 523 K). During the reaction, the spectra are analyzed in terms of the following additional contributions: (i) two sextuplets ($H \simeq 205$ kOe and $H \simeq 138$ kOe) corresponding to a carbide phase $Fe_{2+x}C$ (*12*) and (ii) another paramagnetic component for which the resolution of the spectra is not unique since it can be interpreted either as a single line corresponding to Fe_3O_4, or as a doublet with the isomer shift of a carbide phase which would therefore be superparamagnetic.

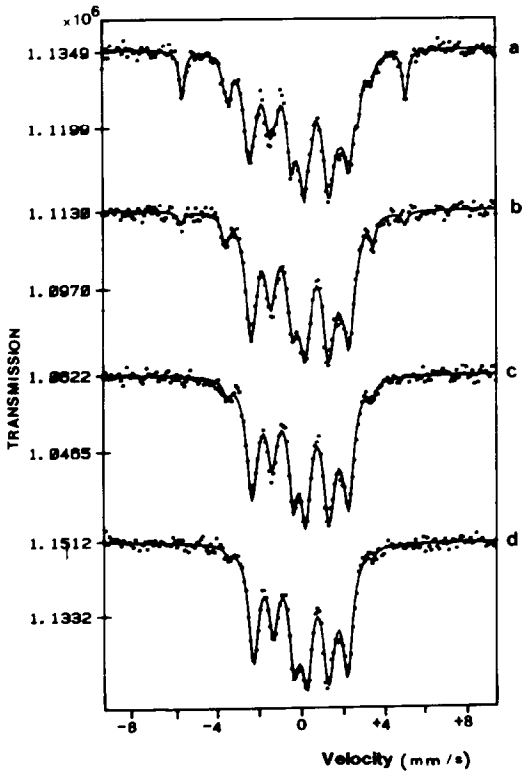

FIG. 3. Mössbauer spectra of the reduced iron/alumina catalyst during the $H_2 + CO$ reaction at 523 K. Spectra recorded at 523 K. (a) 1 h, (b) 3 h, (c) 5 h, and (d) 22 h.

TABLE 1

Mössbauer Parameters at $T = 4$ K of the Ferromagnetic Carbide Obtained after 20 h of Reaction at 523 K

δ (mm s^{-1})	H (kOe)	Spectral contribution (%)
0.67	251.3	10.5
0.68	188.2	62

To assign this component better, a spectrum was recorded at 4 K on a catalyst carburized during 20 h of reaction and transferred into a sealed sample holder. In order to avoid the possibility of air oxidation (to Fe_3O_4) (*17, 18*), we took the precaution of handling the sample in an inert atmosphere in a glovebox. The fit of the 4-K spectrum indicates a ferromagnetic phase with the parameters given in Table 1.

Therefore, the spectra of the catalyst during the reaction fit best with the contribution of a superparamagnetic carbide phase. Table 2 gives the values of the hyperfine parameters of the different phases during the synthesis. The percentage of superparamagnetic carbide increases with time.

In view of the fast change in the catalyst at the start of the reaction, additional data were necessary to study the appearance of the carbide phase. For this purpose, two samples were tempered after 15 and 30 min

TABLE 2

Mössbauer Parameters of Fe/Al_2O_3 Catalysts after Different Periods of Fischer–Tropsch Synthesis at $T = 523$ K (Spectra Recorded at 523 K)

Reaction time (h)	Metallic iron $\delta = 0.15$ mm s^{-1}		Ferromagnetic iron carbide $\delta = 0.36$ mm s^{-1}				Superparamagnetic iron carbide $\delta = 0.35$ mm s^{-1}	
	H (kOe)	Percentage[a]	H_{2C} (kOe)	Percentage[a]	H_{3C} (kOe)	Percentage[a]	Δ (mm s^{-1})	Percentage[a]
0.5	313.0	19.1	204.7	8.1	141.1	42.2	0.55	4.0
1	312.8	11.9	205.0	7.5	140.0	49.7	0.59	4.4
2.6	313.9	3.9	209.3	6.5	138.7	58.2	0.56	6.5
3.2	313.7	3.4	208.0	6.3	138.1	58.7	0.54	6.1
4.6			201.6	5.8	136.8	62.5	0.54	6.4
5.2			204.0	5.2	136.1	63.4	0.54	7.4
6.6			206.8	4.1	135.9	62.5	0.50	8.4
21			200.4	2.8	132.3	64.0	0.54	10.1
22			202.7	2.2	132.6	62.3	0.57	10.0
22[b]			235.4	4.4	172.6	54.3	0.98	19.7

[a] Spectral contribution.
[b] Spectrum recorded at room temperature.

of H_2 + CO reaction at 523 K, and their spectra were taken at room temperature. The fits of the spectra are shown in Fig. 4. After only 15 min of reaction, ~40% of the initial metallic iron has been transformed. Even if this value is overestimated due to the fact that the reaction has been going on for several minutes during the cooling down, it is clear that the carburization is a very fast process. The superparamagnetic carbide components of these two spectra should not be studied together with the similar components of the other spectra, since they should be ascribed to the small domains of carbide growing inside larger iron grains.

3.3. Evolution of the Catalyst Composition during the Fischer–Tropsch Reaction

The spectral contributions of the different phases during the reaction, namely Fe^{2+}, α-Fe, and iron carbides, are represented in Fig. 5. The precision is better than that indicated by the size of the symbols. This clearly appears by considering in Table 2 the compositions obtained for the spectra recorded after 21 and 22 h at 523 K.

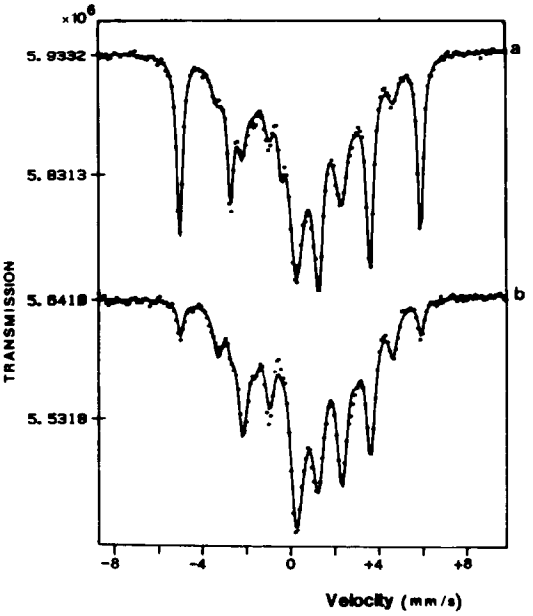

FIG. 4. Mössbauer spectra of tempered iron/alumina catalysts after (a) 15 min and (b) 30 min of H_2 + CO reaction at 523 K. Spectra were recorded at room temperature.

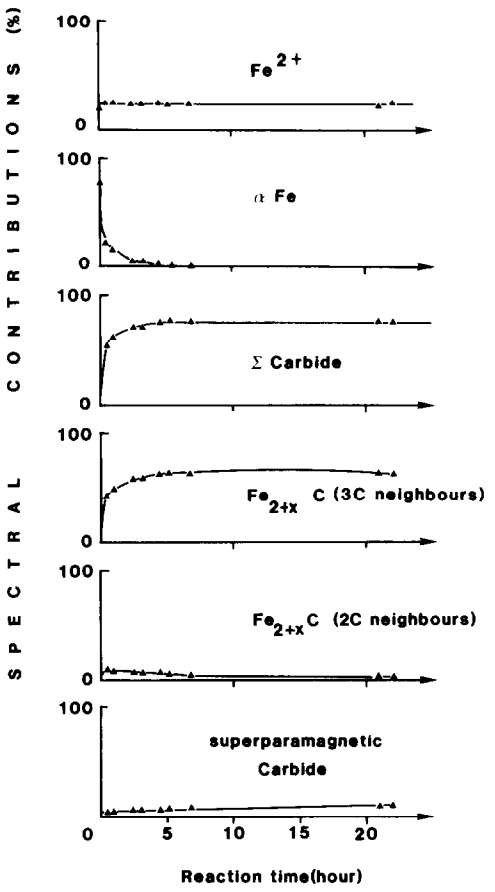

FIG. 5. Changes in the phases of Fe/Al_2O_3 catalyst in the course of Fischer–Tropsch reaction at 523 K.

Ferrous Iron

This species, present in the reduced catalyst, could be attributed to wüstite $Fe_{1-x}O$, in view of the value of the isomer shift together with the large linewidth. In this case, the large value of the quadrupolar splitting (~1.6 mm s^{-1} instead of 0.5 and 0.7 for $Fe_{1-x}O$) would indicate that this phase is present as very small particles. Another interpretation of this doublet could be Fe^{2+} ions in strong interaction with alumina (*19*). It is not possible to conclude to what species this spectral component must be ascribed. However, the concentration of this ferrous iron is nearly unchanged during the reaction.

Metallic Iron

After 4 h of reaction, no metallic iron is detected. To be certain of the absence of metallic iron after 20 h of synthesis, a spectrum was recorded at room temperature during 48 h to a counting level of $\sim 30.10^6$. For this spectrum, it would have been possible to detect a concentration of metallic iron as low as ~1%. However, no fit could be found by introducing either the sextuplet of metallic iron or a line corresponding to superparamagnetic metallic iron. Consequently there remains no metallic iron, even if we cannot exclude the existence of surface zones of metal atoms, considering the low initial metallic dispersion of the catalyst (2–3%, see Ref. (*14*)).

Iron Carbides

In a previous paper (*12*), we have discussed the formation of carbides in this Fe/Al_2O_3 system. These "O carbides," i.e., with carbon atoms in octahedral interstices, present two hyperfine magnetic fields H_{2C} ~ 240 kOe and H_{3C} ~ 170 kOe at room temperature, corresponding to Fe atoms with two and three carbon atoms as nearest neighbors, respectively. From the areas of the H_{2C} and H_{3C} spectral components, it is easy to obtain the value of x in the carbide $Fe_{2+x}C$, according to the previously established formula (*12*)

$$6/(2 + x) = 3\,p_{\mathrm{I}} + 2\,p_{\mathrm{II}},$$

where p_{I} and p_{II} are the respective populations of the iron sites giving the two hyperfine magnetic fields H_{3C} and H_{2C}.

Figure 6 represents the variations of x versus the time of reaction. At the beginning of the synthesis, the carbide stoichiometry is close to $Fe_{2.2}C$ (spectra in Fig. 4: $Fe_{2.23}C$ after 15 min and $Fe_{2.2}C$ after 30 min). As metallic iron disappears the carbide is progressively enriched in carbon and approaches the Fe_2C stoichiometry. This explains the decrease in the number of iron atoms with two carbon neighbors in Fig. 5 and Table 2.

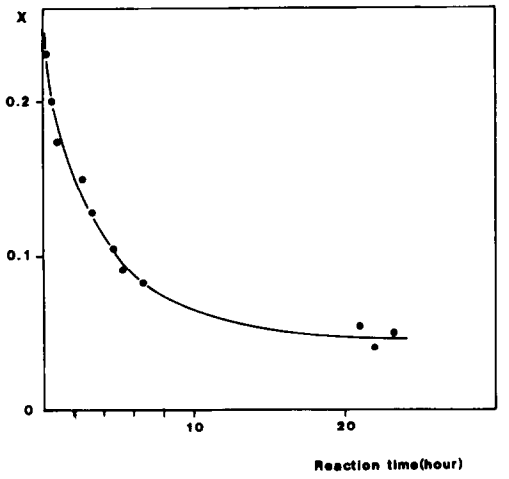

FIG. 6. Variation of the $Fe_{2+x}C$ carbide stoichiometry: x vs time of reaction. $T = 523$ K.

The stoichiometry of the superparamagnetic carbide is uncertain. However, since the concentration of this phase varies as does that of the ferromagnetic carbide, their stoichiometries are probably similar. This implies the existence of different-size particles of carbides, some of which are in the paramagnetic state.

3.4. Relation between the Carbide Stoichiometry and the Catalytic Activity in the Fischer–Tropsch Synthesis at 523 K

Many authors have agreed within the last few years that the catalytic activity in the FT synthesis is related to the formation of active surface carbon (*20–22*) rather than to that of bulk carbide (*9–11*). Thus, Niemantsverdriet and van der Kraan (*21*) have proposed a "competition model" in which the carbon species from CO dissociation can react either with Fe to give carbides or with hydrogen atoms to give intermediates for hydrocarbon formation. The rates of these two reactions can be different depending on the contact mass and the reaction conditions, and consequently a maximum can be induced in the hydrocarbon production.

With our Fe/Al_2O_3 catalyst, the surface carbon layer is formed very quickly for $T > 498$ K since the initial activity curve decreases with time. This is in agreement with the observations of Tau *et al.* (*23*) who have shown that a similar Fe/Al_2O_3 contact mass adsorbs no CO at room temperature after 20 s of reaction at 558 K. However, at 473 K, an induction period is observed (Fig. 1) which is due to the competition between hydrogenation and carburization.

In this study, we have investigated the case where the surface is quickly covered with carbon (at 523 K). In Fig. 5, it was shown that the bulk is also carbided in a few hours whilst the activity decreases sharply. A question arises from these two observations: which sites are responsible for the residual activity?

Two hypotheses can be proposed: (i) there exists a small number of superficial zones of metallic iron, free of carbon; the activity decrease would result from a poisoning due to the covering of these zones by "less reactive" carbon. (ii) The surface is that of a $Fe_{2+x}C$ carbide whose activity varies inversely with its carbon content.

Concerning the first hypothesis, the Mössbauer spectroscopy is not conclusive (see previous section). However, *in situ* IR spectroscopy of the CO adsorption on a used catalyst (when the reaction is performed at atmospheric pressure) did not reveal any CO absorption band characteristic of CO associated with the iron in the metallic state (*16*). Consequently, it seems that the superficial metallic iron may not exist after 20 h of reaction, unless in a concentration too low to be consistent with the residual activity.

Figure 7 supports the second hypothesis. It shows the evolution of the activity versus the composition of the iron carbide $Fe_{2+x}C$. A linear variation is observed for $x > \sim 0.06$, i.e., for carbides with a larger number of carbon vacancies. For $x < \sim 0.06$, i.e., when the carbide is close to the stoichiometry, the activity decreases very quickly with x. One may ask whether a carbide

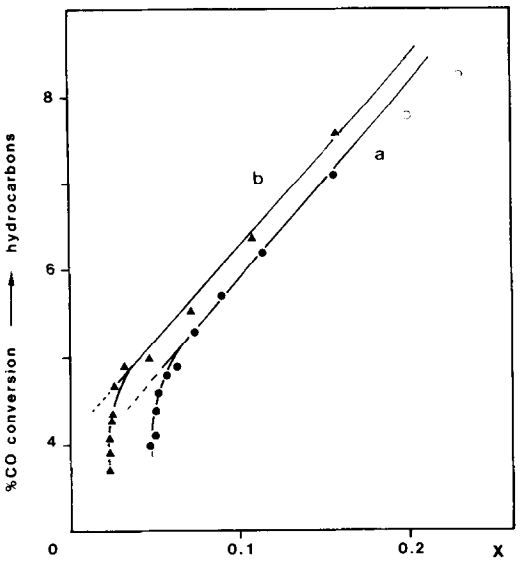

FIG. 7. Change of the activity from the H_2 + CO reaction at 523 K as a function of the $Fe_{2+x}C$ stoichiometry. (●, ○) Fe/Al_2O_3, (▲) $Fe–Cr/Al_2O_3$. x was determined from *in situ* Mössbauer spectra at 523 K, except for two spectra (○) recorded at room temperature.

corresponding exactly to the Fe_2C stoichiometry is active. Other studies would be necessary to answer this question.

A similar correlation was sought for a chromium-promoted iron catalyst. This contact mass was prepared by impregnating the initial Fe/Al_2O_3 precursor with $(NH_4)_2Cr_2O_7$. The catalytic activity was found to be very close to that of Fe/Al_2O_3, and a comprehensive Mössbauer study was performed (*12*). Effectively, curve b in Fig. 7 indicates a similar linear variation of the activity vs the composition of the iron carbide. Thus it can be deduced that the activity of these iron catalysts in the CO hydrocondensation increases with the number of carbon vacancies in the iron carbide. This property may in turn be related to the change of the metallic character of the carbide with the carbon content, as discussed in the Introduction.

To prove this concept, it was necessary to test several $Fe_{2+x}C$ carbides of different compositions in another hydrogenation reaction and to examine the variation of the activity with the number of carbon vacancies. To avoid chemical transformation resulting from too high a reaction temperature, the ethylene hydrogenation at room temperature was chosen. The results are presented and discussed in the next section.

3.5. Ethylene Hydrogenation

The carbides were prepared *in situ* in the reactor by performing the H_2 + CO reaction at 523 K during selected times. The resulting contact masses were cooled to room temperature. The stoichiometry of the carbide was calculated from the Mössbauer results. TPR under H_2 were performed after the ethylene hydrogenation to check the quantity and the type of the carbon content. These values, though approximate due to formates and carboxylates present on the support (*16*), were consistent with the carbon content calculated by Mössbauer measurements. Moreover, the methane TPR peak presented only a negligible drift in the high temperature region (650–800 K) but no peak was attributable to less reactive (or poisoning) carbon, as could be observed after FT synthesis at 548 K (*16*). The reaction temperature was 305 K. Several preliminary experiments were necessary to ascertain the reproducibility of the reaction conditions. Thus it was shown that after the carburization in the FT reaction the gaseous atmosphere (He or H_2 + CO) during the cooling from 523 to 305 K had no direct influence on the subsequent hydrogenation activity. However, the latter was dependent on traces of CO in the H_2 + C_2H_4 mixture. Indeed it was observed that pulses of CO (400 ppm) during a few minutes killed the hydrogenation activity which was subsequently restored very slowly. To limit this poisoning effect, the reactor was thoroughly purged with helium (~15 h) before introducing the H_2 + C_2H_4 mixture. Nevertheless, in most cases, an initial increase in activity was observed followed by a gradual

decrease. The maximum values were chosen to compare the hydrogenation activities.

Moreover, under our conditions alumina alone was active in ethylene hydrogenation. After H_2 activation at 873 K, the conversion to ethane was ~5%, whereas it was ~3% after 15 h of H_2 + CO at 523 K. Thus we can consider that the contribution of the support is negligible compared to the conversion of 100% for the initial reduced catalyst.

Figure 8 represents the ethylene hydrogenation activity of different carbided catalysts versus the corresponding activity in hydrocarbon formation from H_2 + CO. It is obvious that in the range 4–6% of conversion into hydrocarbons, there is a close relation between these two reactions. It would be necessary to operate the ethylene hydrogenation at much lower temperatures to enlarge the validity range to the more active (less carbided) catalysts. However, from Figs. 7 and 8, it can be deduced that the hydrogenation activity of carbided iron in the H_2 + C_2H_4 as well as in the H_2 + CO reaction progressively decreases as the stoichiometry becomes closer to Fe_2C. Since the mechanisms are not the same in the two reactions, this emphasizes the importance of the carbon vacancies of the transition metal carbides on their hydrogenation capacity and consequently on their catalytic activity. This result is in agreement with the observation of Jensen and Massoth (*24*) who noticed that carburization decreases the hexene hydrogenation activity of iron–manganese catalysts.

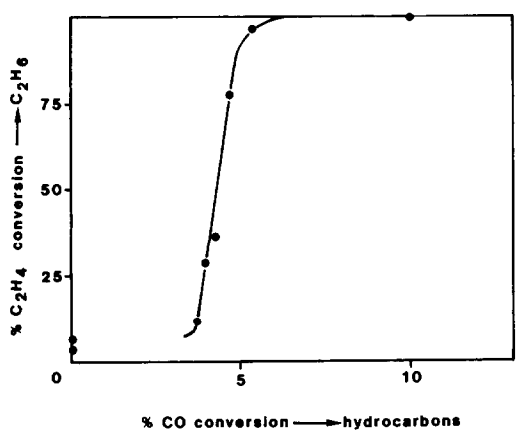

FIG. 8. Comparison of the activities of different carbided iron/alumina catalysts in H_2 + C_2H_4 (T = 305 K) and H_2 + CO (T = 523 K) reactions.

4. CONCLUSION

Extensive work has already been devoted to the study of the different forms of carbon present on the surface of iron catalysts and their role in hydrocarbon production. The present study was focused on the variation of the hydrogenation capability of the catalytic contact mass as a function of the reaction time.

From a precise physicochemical characterization of the system, we have shown that the loss of hydrogenation activity (toward CO and ethylene) is directly related to the loss of the iron metallic character, occasioned by the progressive carbon enrichment of the $Fe_{2+x}C$ iron carbide. This relation exists insofar as the carbon atom distribution in the carbide is homogeneous. Obviously it is not valid at higher temperatures where other types of carbide are favored and under conditions where less reactive or poisoning carbon deposits occur on the surface. Nevertheless, this work shows that the activity in Fischer–Tropsch synthesis is related not only to the formation of the surface carbidic phase but also to its evolution in the bulk.

ACKNOWLEDGMENTS

We wish to thank CNRS (GRECO Oxydes de carbone) for financial support and Drs. R. P. A. Sneeden and M. Primet for fruitful discussions.

REFERENCES

1. Levy, R. B., *in* "Advanced Materials in Catalysis" (J. J. Burton and R. L. Garten, Eds.), p. 101. Academic Press, New York, 1977.
2. Oyama, S. T., and Haller, G. L., Spec. Per. Rep. "Catalysis," Vol. 5, p. 333. Royal Society of Chemistry, London, 1982.
3. Leclercq, L., *in* "Surface Properties and Catalysis

by Non-Metals" (J. P. Bonnelle, B. Delmon, and E. Derouane, Eds.), p. 433. Reidel, Dordrecht, 1983.

4. Kharlamov, A. I., Krivitskii, V. P., and Lemeshko, N. D., *React. Kinet. Catal. Lett.* **17,** 63 (1981).
5. Kojima, I., Miyazaki, E., Inoue, Y., and Yasumori, I., *J. Catal.* **73,** 128 (1982).
6. Kharlamov, A. I., Pankratiev, Yu. D., Lemeshko, N. D., and Malyshev, E. M., *React. Kinet. Catal. Lett.* **17,** 311 (1981).
7. Amelse, J. A., Butt, J. B., and Schwartz, J., *J. Phys. Chem.* **82,** 558 (1978).
8. Raupp, G. B., and Delgass, W. N., *J. Catal.* **58,** 348, 361 (1979).
9. Matsumoto, H., and Bennett, C. O., *J. Catal.* **53,** 331 (1978).
10. Dry, M. E., *in* "Catalysis" (J. R. Anderson and M. Boudart, Eds.), Vol. 1, p. 159. Springer-Verlag, New York/Berlin, 1981.
11. Sommen, A. P. B., Stoop, F., and van der Wiele, K., *Appl. Catal.* **14,** 277 (1985).
12. Le Caër, G., Dubois, J. M., Pijolat, M., Perrichon, V., and Bussière, P., *J. Phys. Chem.* **86,** 4799 (1982); Pijolat, M., Le Caër, G., Perrichon, V., and Bussière, P., *in* "Int. Conf. on the Applications of the Mössbauer effect, Jaïpur, 1981" (Indian Nat. Science Academy, Ed.), New Delhi, 1982.
13. Pijolat, M., Thesis, Lyon, 1983.
14. Nahon, N., Perrichon, V., Turlier, P., and Bussière, P., *React. Kinet. Catal. Lett.* **11,** 281 (1979).
15. Pijolat, M., and Perrichon, V., *C.R. Acad. Sci. Ser. 2* **295,** 343 (1982).
16. Perrichon, V., Pijolat, M., and Primet, M., *J. Mol. Catal.* **25,** 207 (1984).
17. Amelse, J. A., Grynkewich, G., Butt, J. B., and Schwartz, L. H., *J. Phys. Chem.* **85,** 2484 (1981).
18. Nahon, N., Perrichon, V., Turlier, P., and Bussière, P., *in* "Magnetic Resonance in Colloid and Interface Science" (J. P. Fraissard and H. A. Resing, Eds.), p. 377. Reidel, Dordrecht, 1980.
19. Perrichon, V., Charcosset, H., Barrault, J., and Forquy, C., *Appl. Catal.* **7,** 21 (1983).
20. Krebs, M. J., Bonzel, H. P., and Gafner, G., *Surf. Sci.* **88,** 269 (1979).
21. Niemantsverdriet, J. W., and van der Kraan, A. M., *J. Catal.* **72,** 385 (1981).
22. Dwyer, D. J., and Hardenberg, J. H., *J. Catal.* **87,** 66 (1984).
23. Tau, L. M., Bianchi, D., and Bennett, C. O., *J. Catal.* **89,** 533 (1984).
24. Jensen, K. B., and Massoth, F. E., *J. Catal.* **92,** 109 (1985).